18. PHYSICAL PROPERTIES

A. C. Pimm, Scripps Institution of Oceanography, La Jolla, California

This chapter has two limited objectives as follows:

1) To graphically summarize various physical and chemical properties for each site and show their relationship to other important parameters such as lithology, diagenesis, authigenesis and acoustic character.

2) To illustrate at the section (150 cm) level how some physical properties respond to important cyclical variations in lithology and also to some major stratigraphic boundaries. These variations in the physical properties were too subtle to be recorded in the data presentation for each site.

Figures 1 through 9 and downhole summaries of various physical and chemical properties. Tables 1 and 2 list the first occurrences of lithified sediments and some authigenic minerals, respectively. It must be emphasized here, that no firm conclusions should be drawn from these figures and tables because of the scarcity of data points due to spot coring. Furthermore, major hiatuses were detected at Sites 135, 136, and 140, and small hiatuses at Site 144; other hiatuses may also exist at other sites, but the cored data are insufficient to detect them (see site reports and Chapter 27). The duration of the hiatuses cannot always be accurately determined and no reliable estimate can be made of the amount of sediment that may have been removed by erosion during the time represented in the hiatuses.

Despite the uncertainties mentioned above, it is hoped that the presentation of this data for Leg 14 will be useful for integration into future studies based on the results from many of the DSDP cruises.

Figures 10 through 17 show the natural gamma radiation (counts/7.6 cm/1.25 minutes) and porosity (%), and in some cases wet bulk density (gm/cc) on analog graphs adjacent to the section photographs. Where the composition of the sediment is listed under percent of components, these data were obtained from the visual smear slide estimates made on board. X-ray diffraction data were kindly provided by Ulrich von Rad (see Chapter 20); the occurrences of components under this category are listed by initials for abundant, common, rare, and trace.

TABLE 1
First Occurrence of Lithified Sediments

Site	Sandstone		Mudstone/Shale		Limestone		Chert	
Number	Depth (m)	Age	Depth (m)	Age	Depth (m)	Age	Depth (m)	Age
135	435	Maestrichtian	565	Cretaceous	565	Cretaceous	565	Cretaceous
136	270	Senonian	–	–	–	–	–	–
137	–	–	–	–	–	–	260	Cenomanian Turonian
138	–	–	260	Cretaceous/Tertiary	–	–	260	Cretaceous/Tertiary
139	610	Miocene	–	–	–	–	–	–
140	–	–	585	Paleocene	–	–	515	Paleocene?
144	–	–	185	Senonian	185	Cenomanian	–	–

TABLE 2
First Occurrence of Authigenic Minerals

Site	Pyrite		Dolomite		Palygorskite[a]		Zeolite[b]	
Number	Depth (m)	Age	Depth (m)	Age	Depth (m)	Age	Depth (m)	Age
135	565	Cretaceous	345[c]	Lower Eocene	345	Lower Eocene	345	Lower Eocene
136	260	Senonian	240	Early Miocene	240	Early Miocene	260[d]	Early Miocene
137	257	Turonian	300	Cenomanian	100	?	166	Upper Cretaceous
138	117	Upper Oligocene	425	Cenomanian	185	Lower Tertiary?	55	Early Miocene
139	570	Lower Miocene	345	Middle Miocene	–	–	–	–
140	201	Early Miocene	315	Middle Eocene	240	Early Oligocene to Late Eocene	–	–
141	–	–	–	–	85	Early Pliocene	–	–
142	–	–	–	–	530	Miocene	455	Miocene
144	143	Upper Paleocene	165	Maestrichtian-Campanian	140	Paleocene	1	Oligocene

[a] palygorskite recovered on Leg 14 is considered to be of authigenic origin (see Chapters 20 and 27).
[b] mostly clinoplitolite
[c] dolomite may be reworked in part
[d] phillipsite

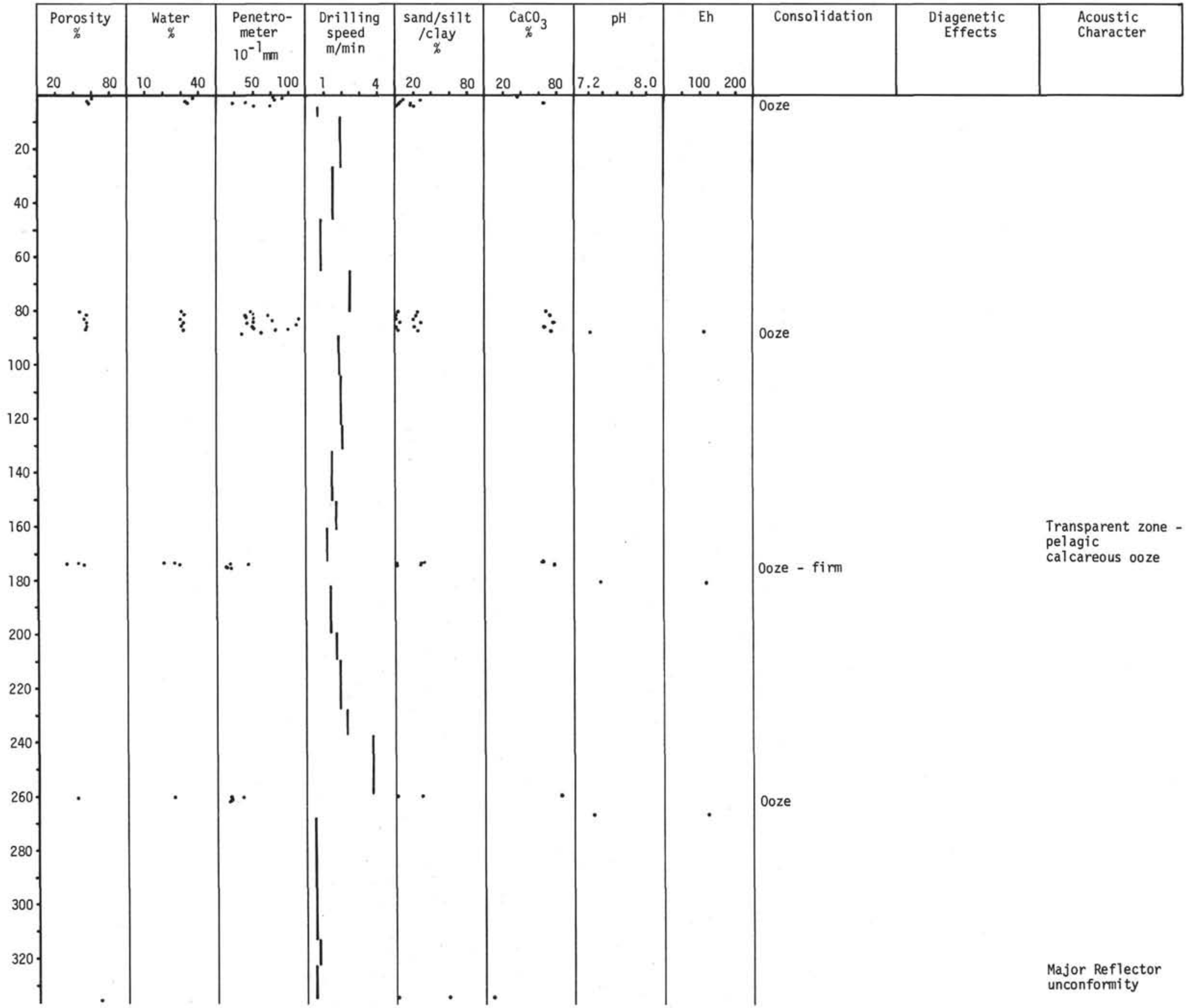

Figure 1. *Site 135.*

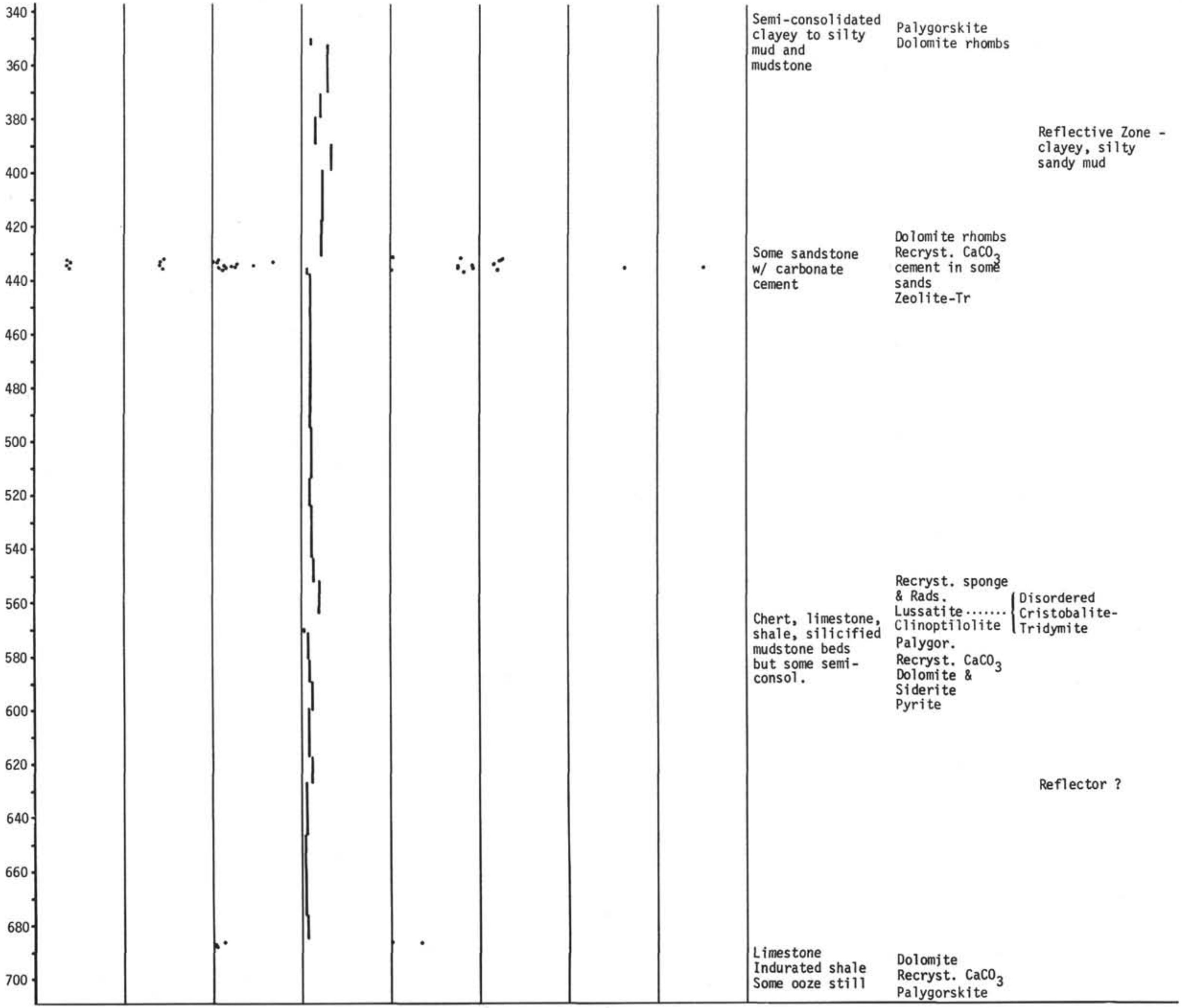

Figure 1. *(Continued).*

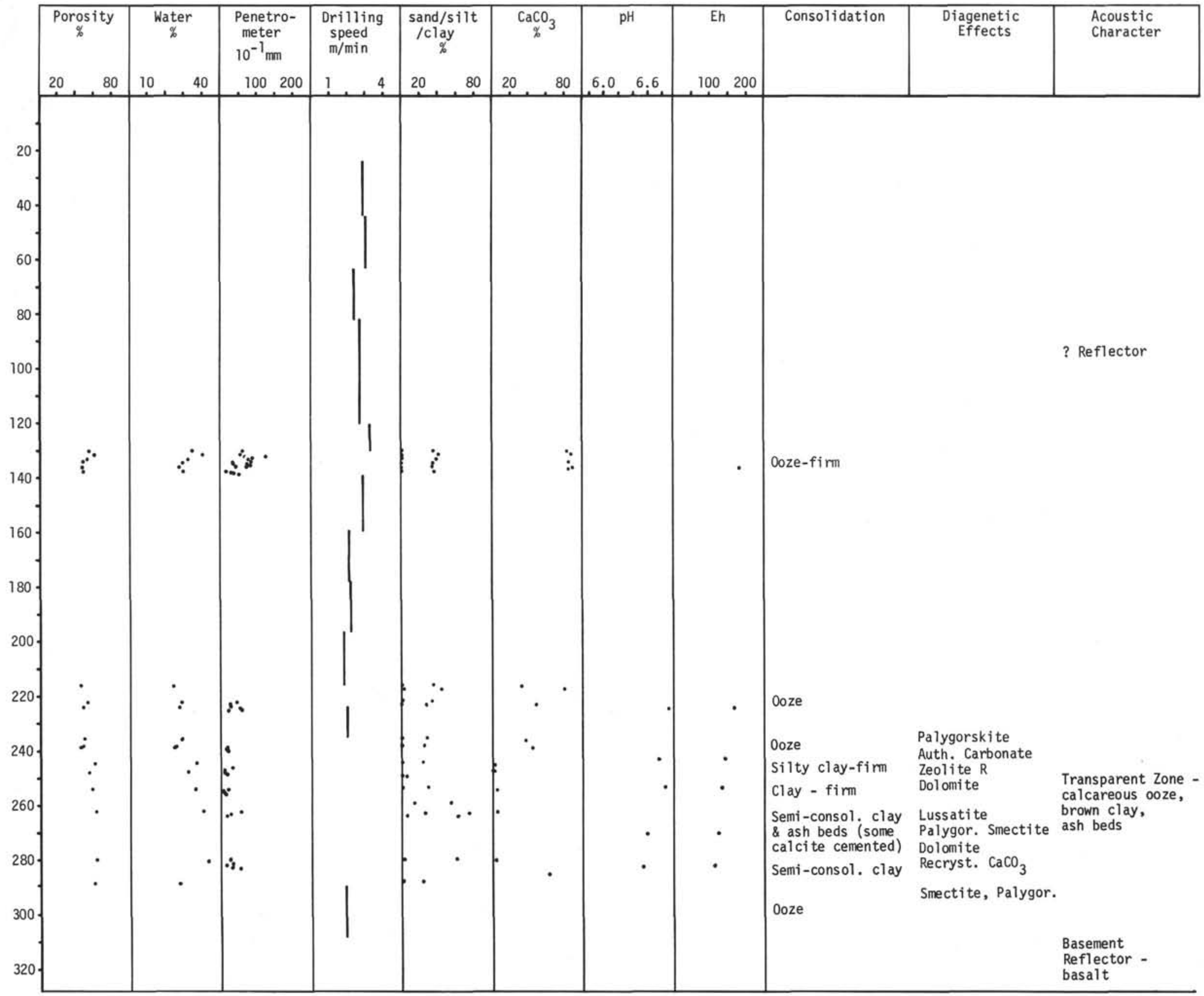

Figure 2. *Site 136.*

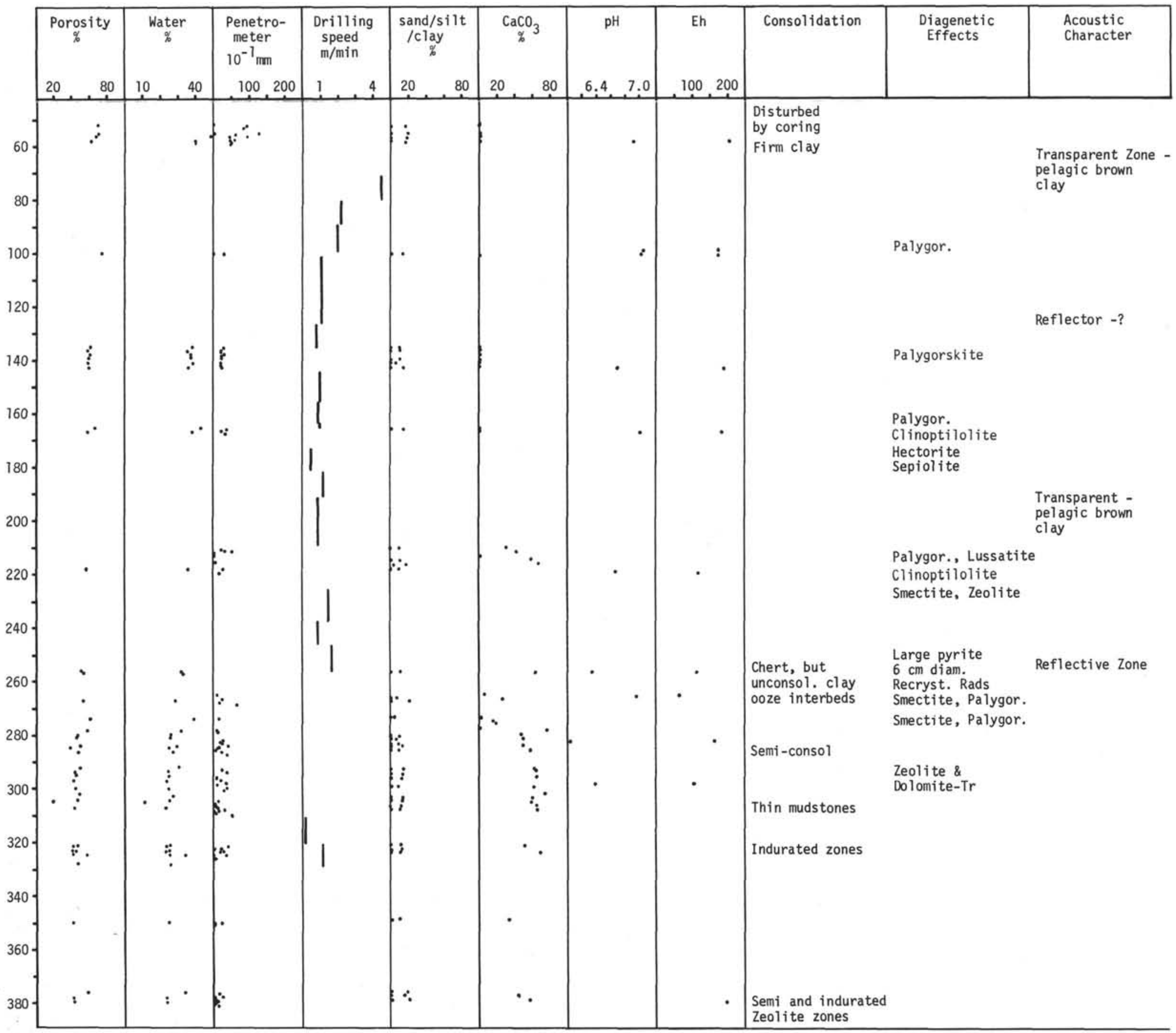

Figure 3. *Site 137.*

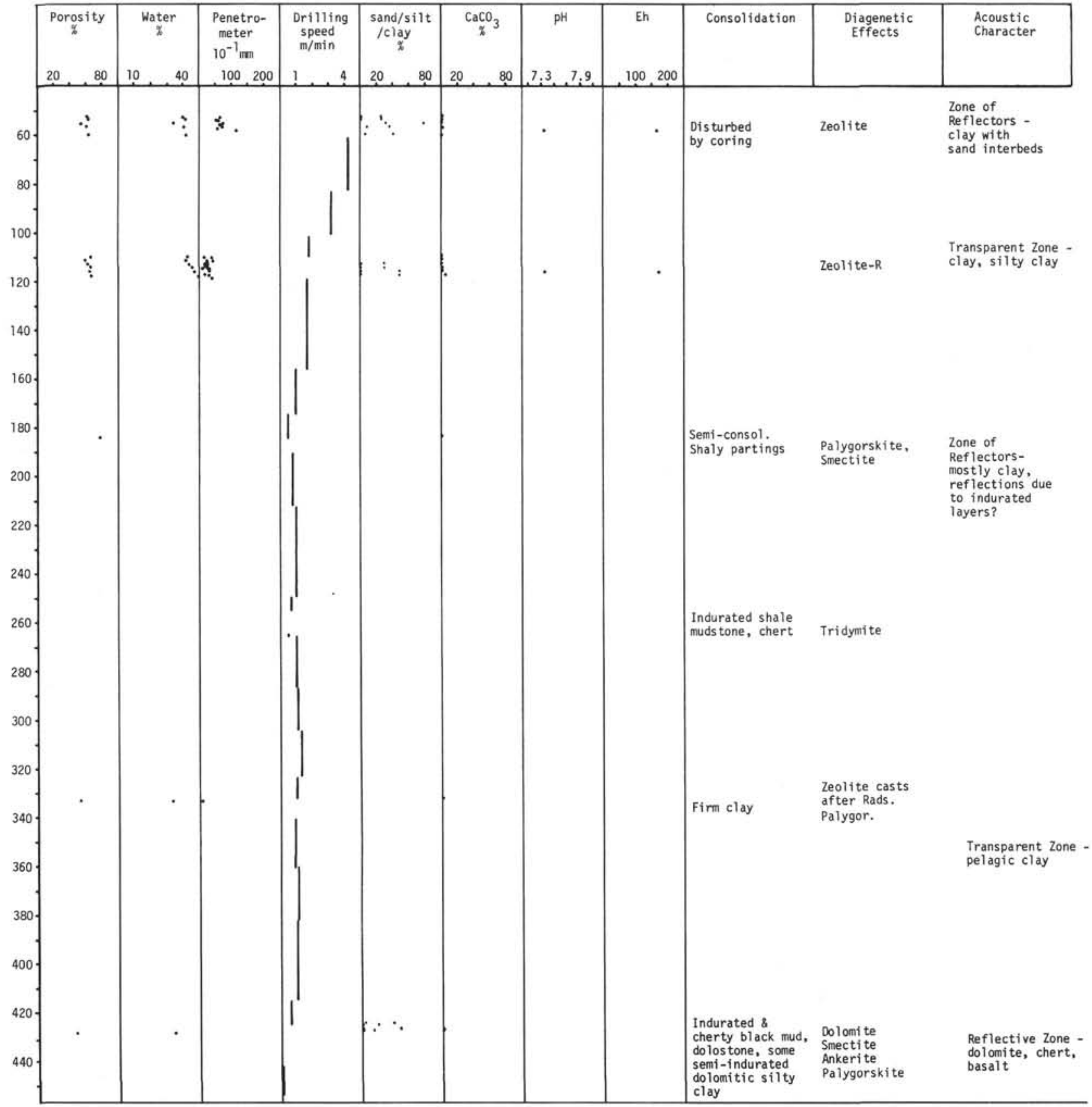

Figure 4. *Site 138.*

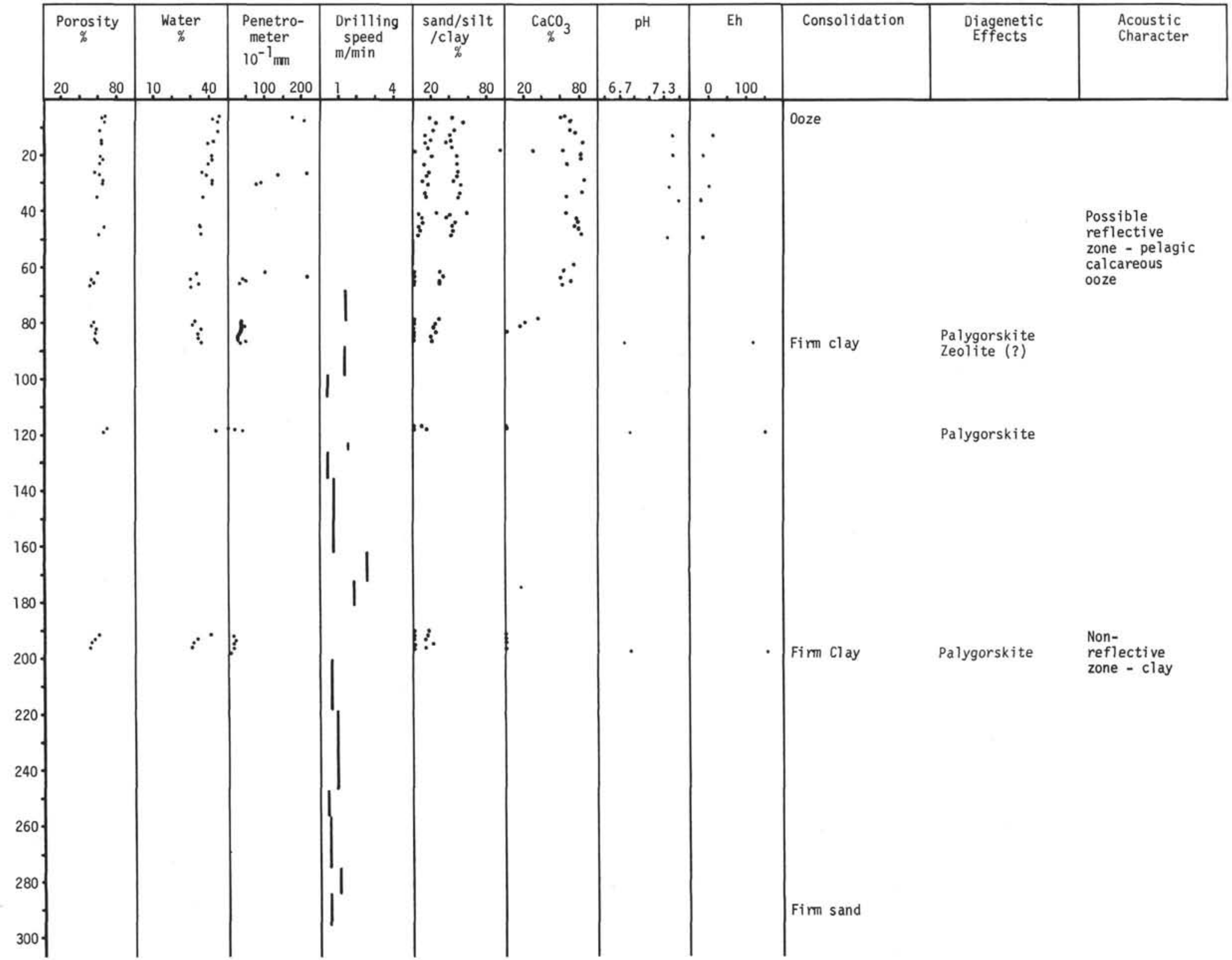

Figure 5. *Site 141.*

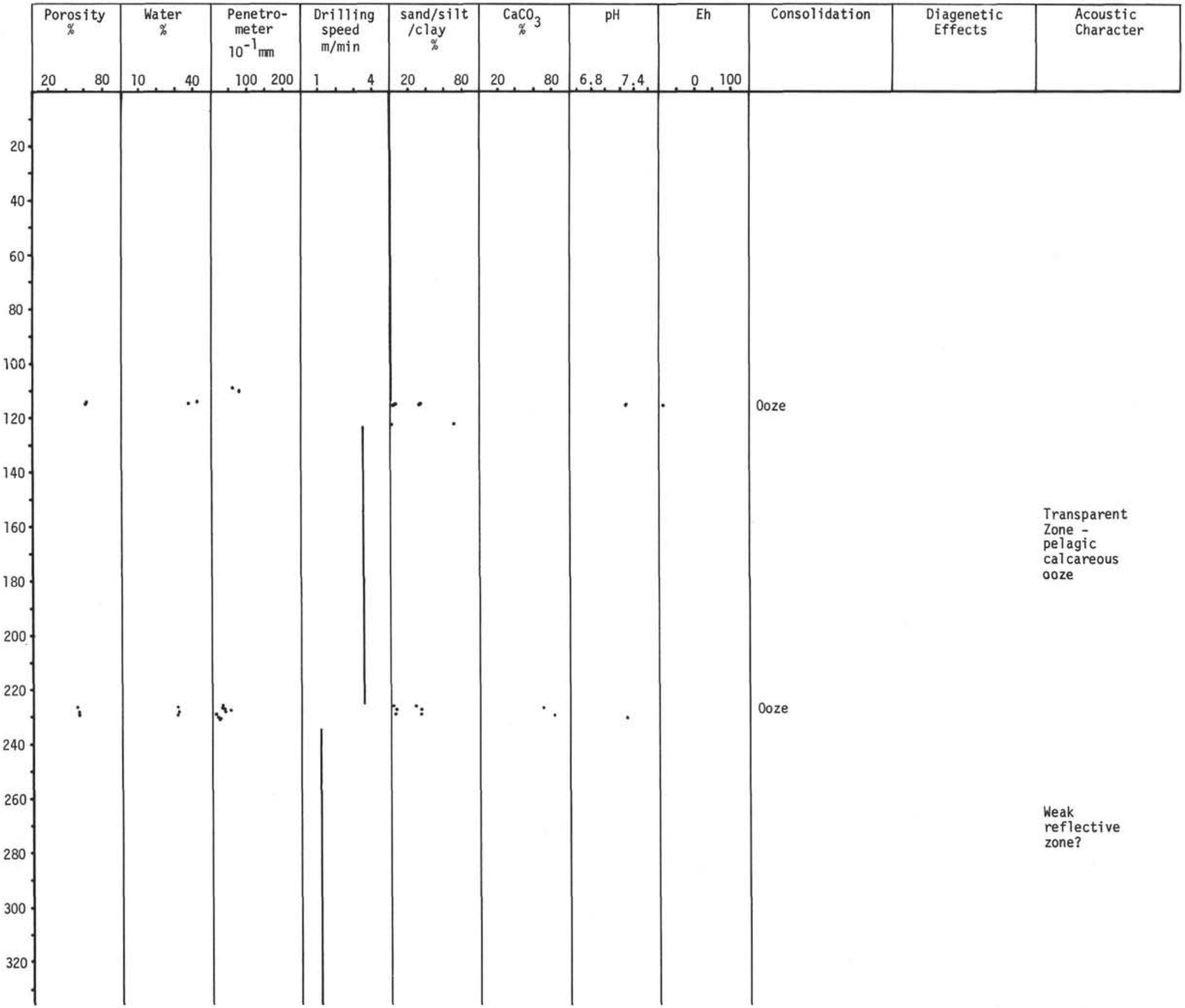

Figure 6. *Site 139.*

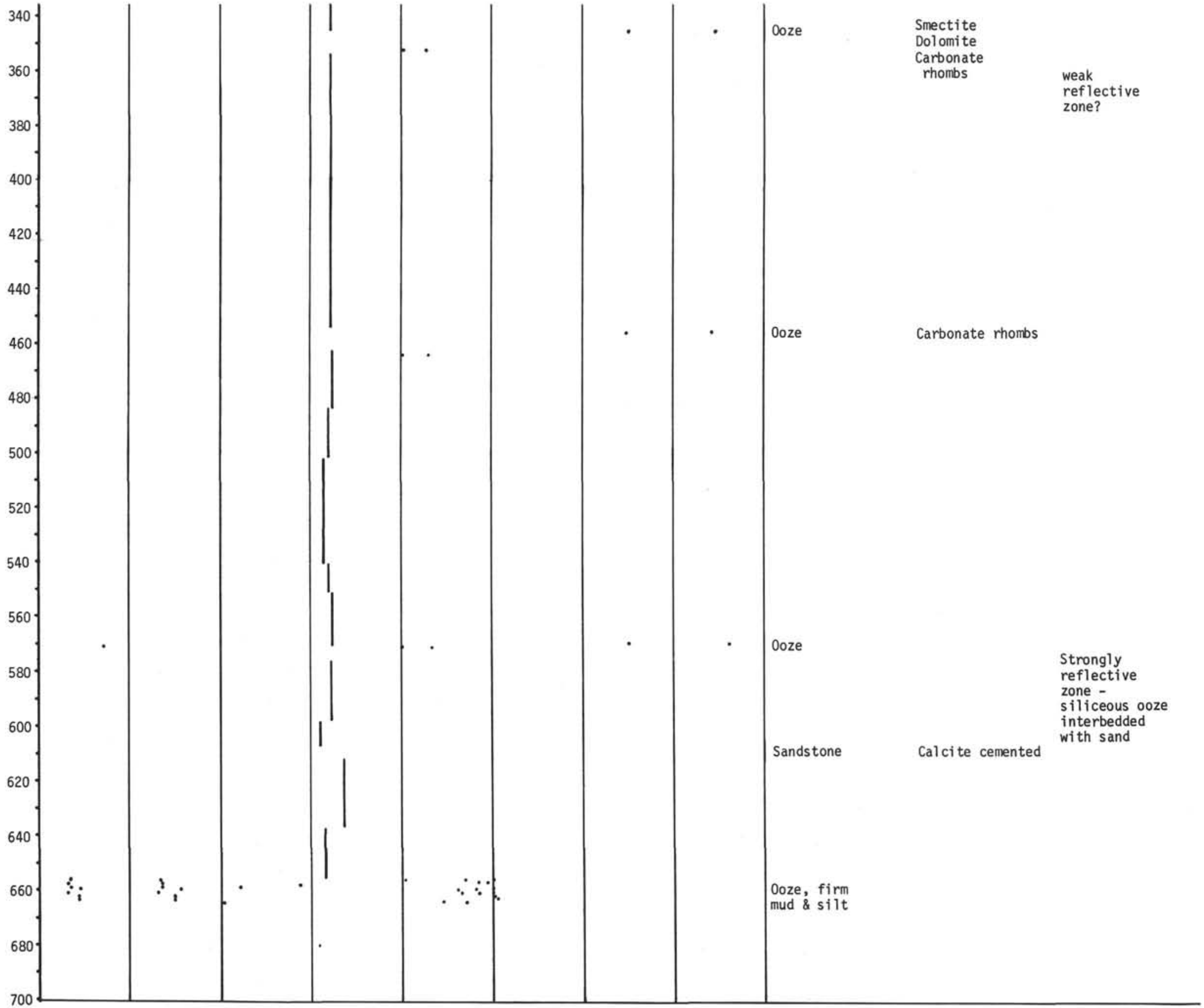

Figure 6. *(Continued).*

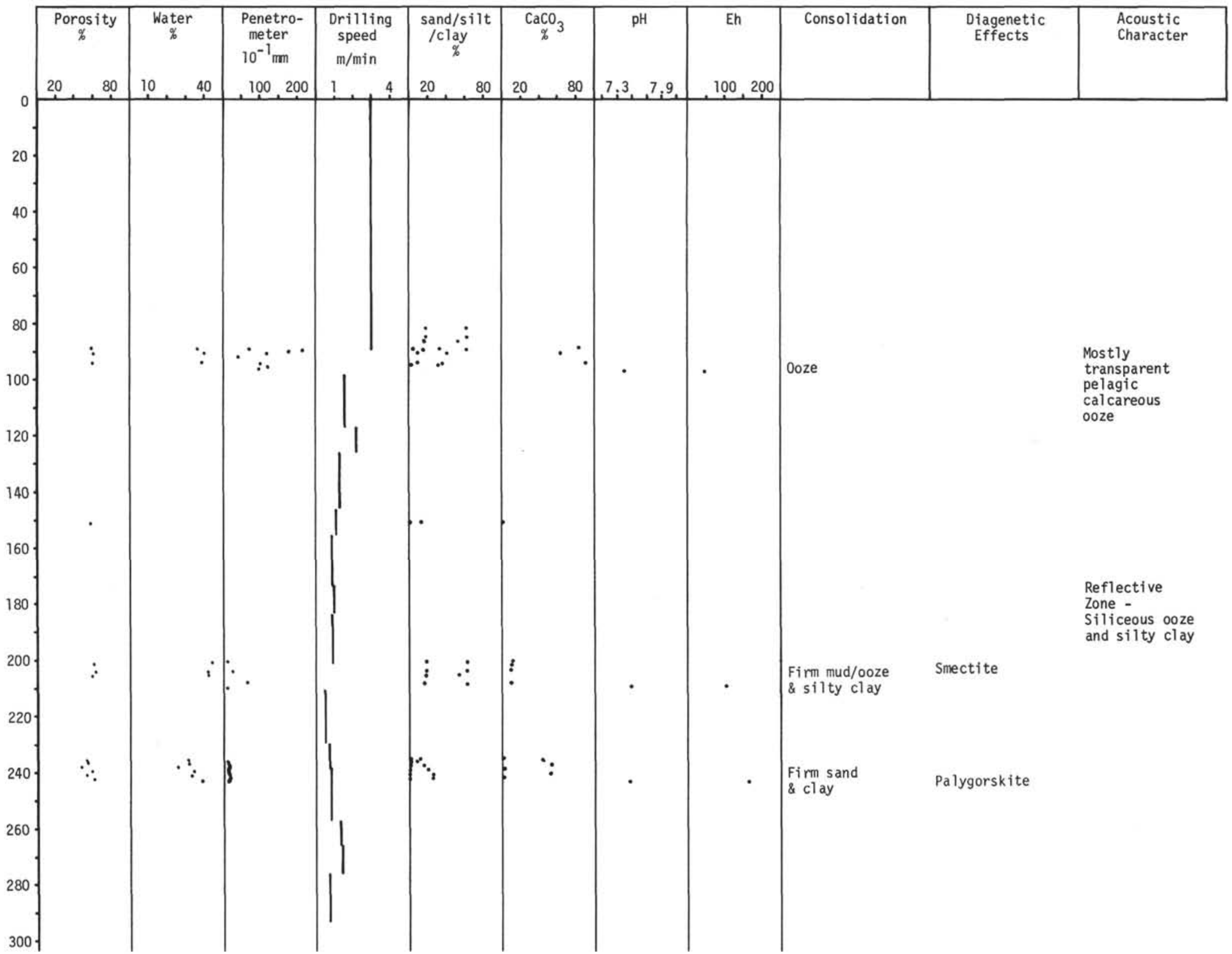

Figure 7. *Site 140.*

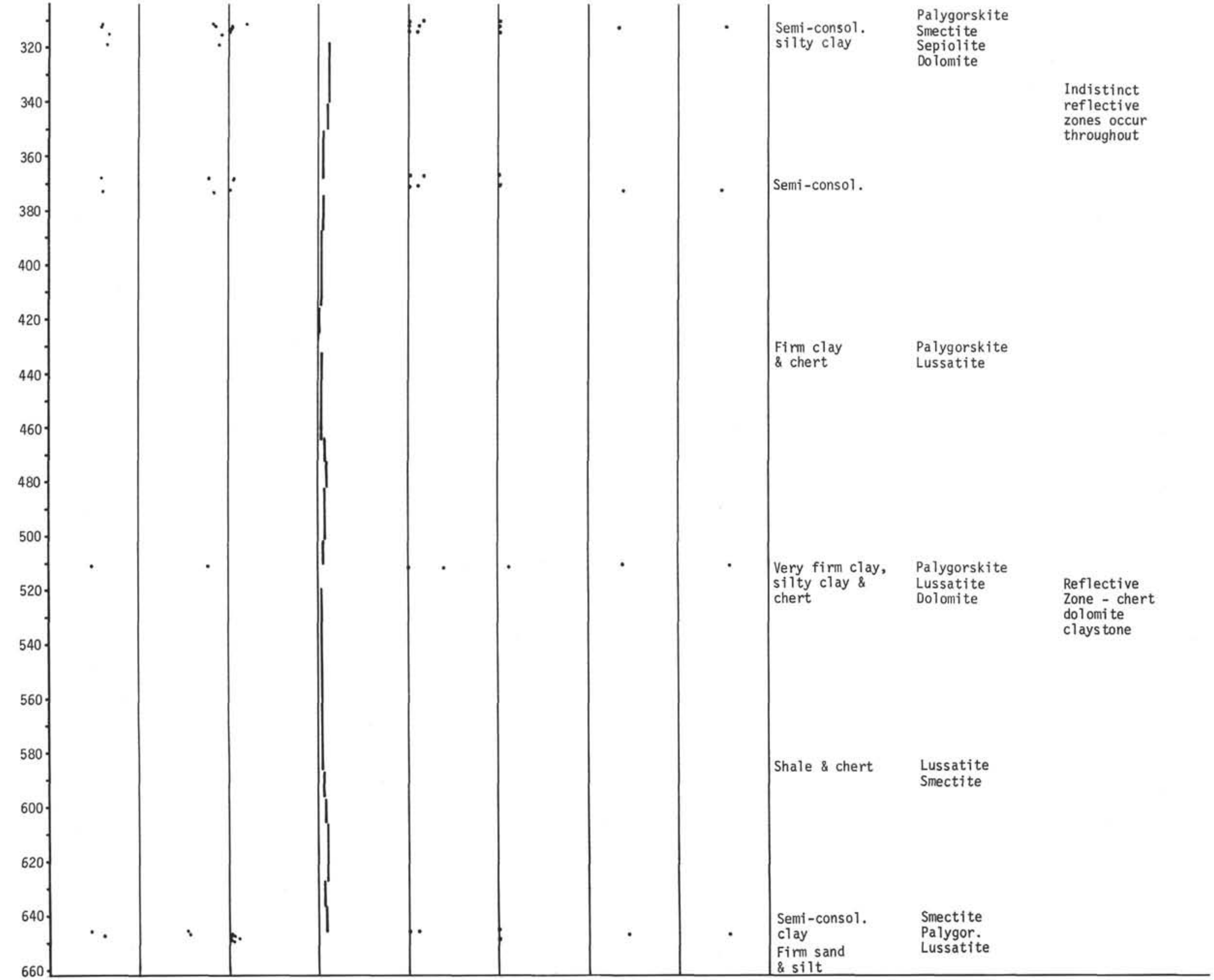

Figure 7. *(Continued).*

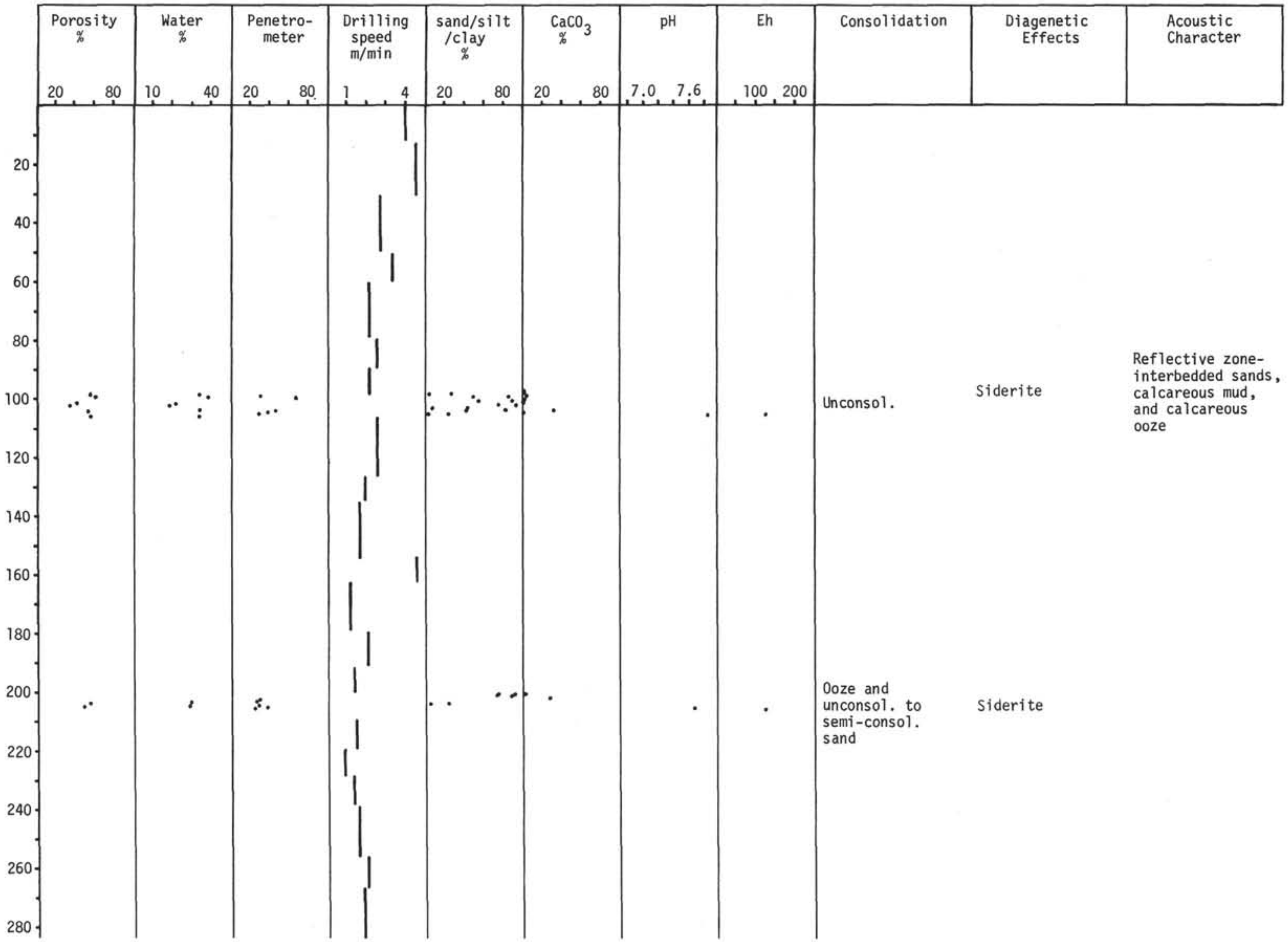

Figure 8. *Site 142.*

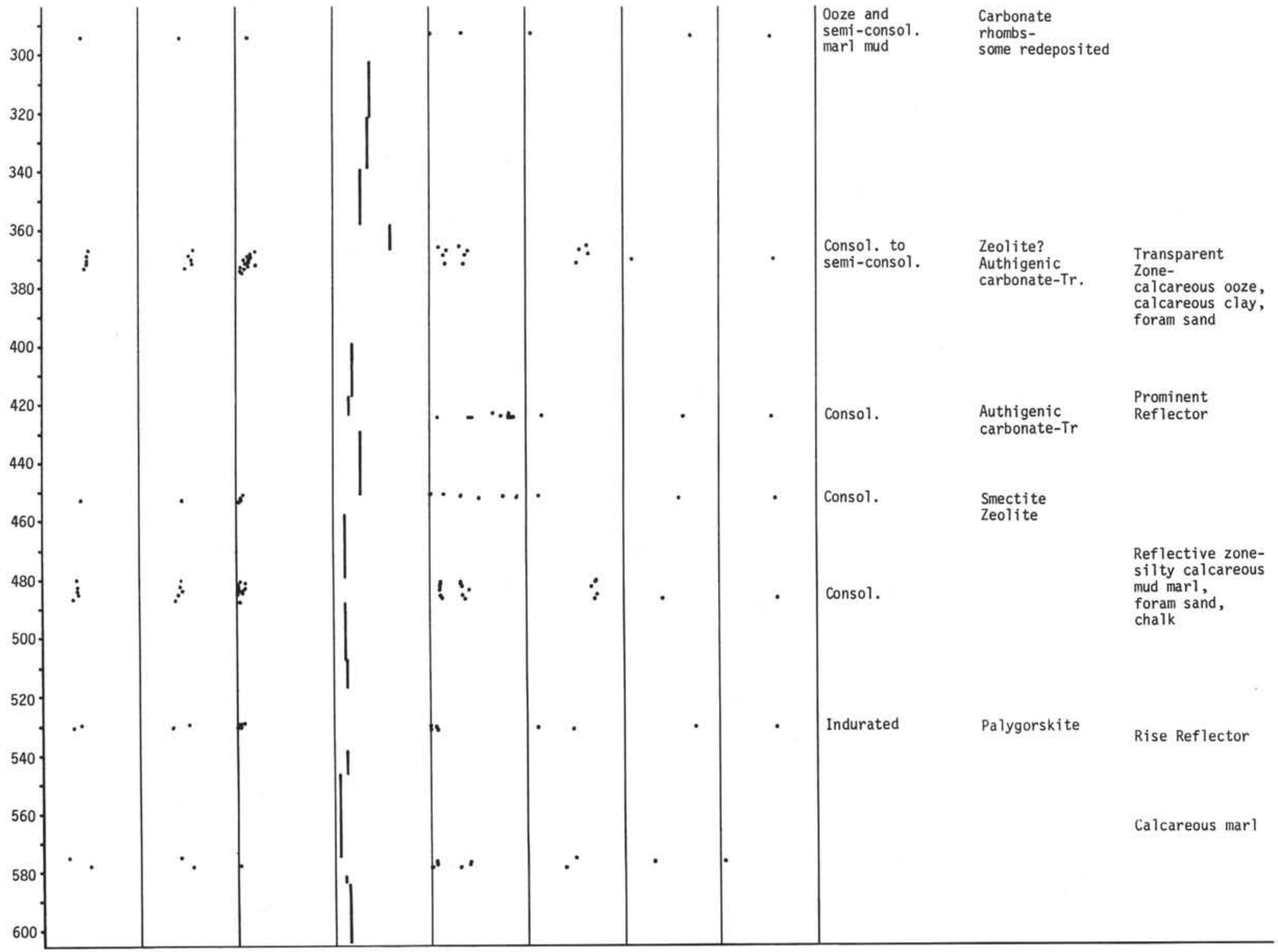

Figure 8. *(Continued).*

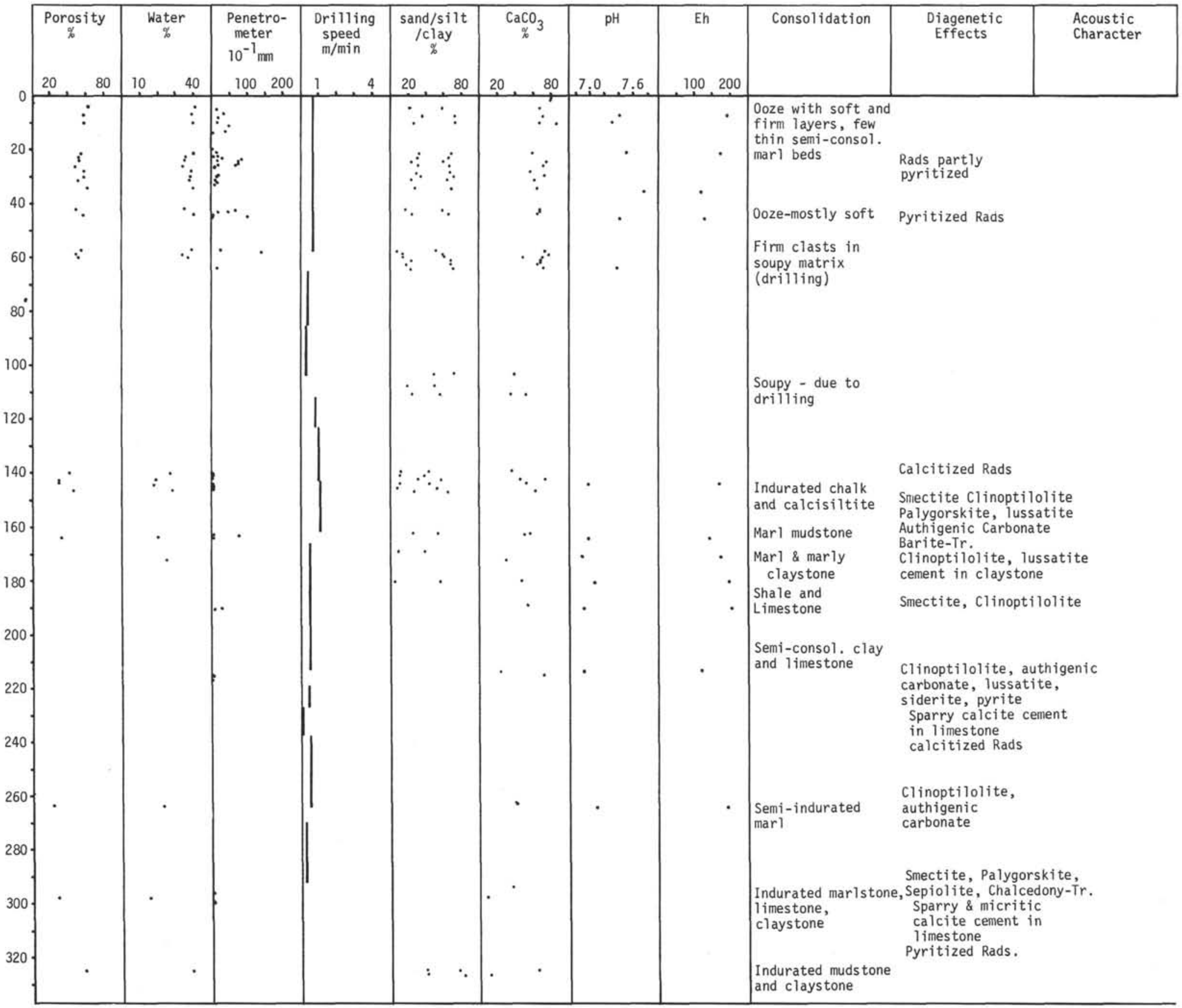

Figure 9. *Site 144.*

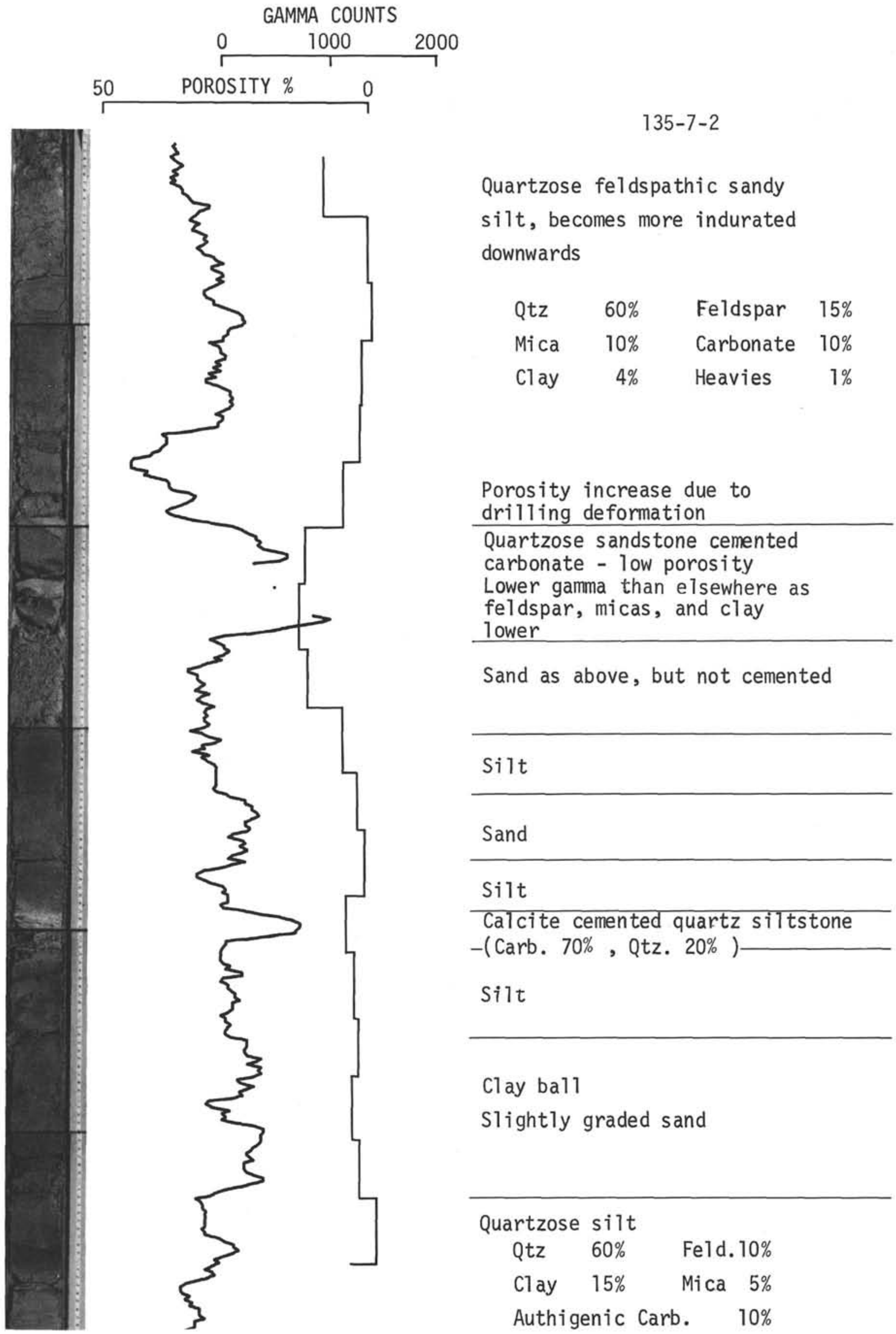
GAMMA COUNTS
0
1000
2000
50
POROSITY %
0
135-7-2
Quartzose feldspathic sandy silt, becomes more indurated downwards
Qtz 60% Feldspar 15%
Mica 10% Carbonate 10%
Clay 4% Heavies 1%
Porosity increase due to drilling deformation
Quartzose sandstone cemented carbonate - low porosity
Lower gamma than elsewhere as feldspar, micas, and clay lower
Sand as above, but not cemented
Silt
Sand
Silt
Calcite cemented quartz siltstone
(Carb. 70% , Qtz. 20%)
Silt
Clay ball
Slightly graded sand
Quartzose silt
Qtz 60% Feld.10%
Clay 15% Mica 5%
Authigenic Carb. 10%

Figure 10.

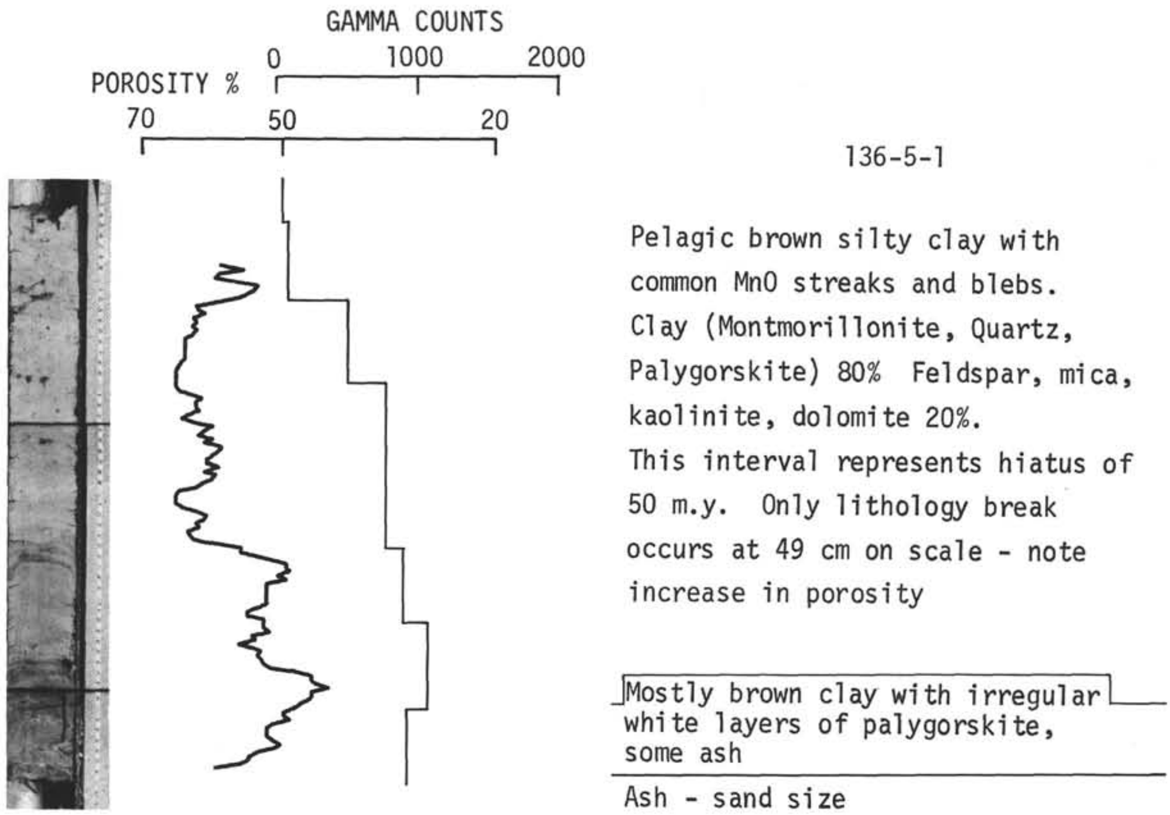
GAMMA COUNTS
0
1000
2000
POROSITY %
70
50
20
136-5-1
Pelagic brown silty clay with common MnO streaks and blebs. Clay (Montmorillonite, Quartz, Palygorskite) 80% Feldspar, mica, kaolinite, dolomite 20%. This interval represents hiatus of 50 m.y. Only lithology break occurs at 49 cm on scale - note increase in porosity
Mostly brown clay with irregular white layers of palygorskite, some ash
Ash - sand size

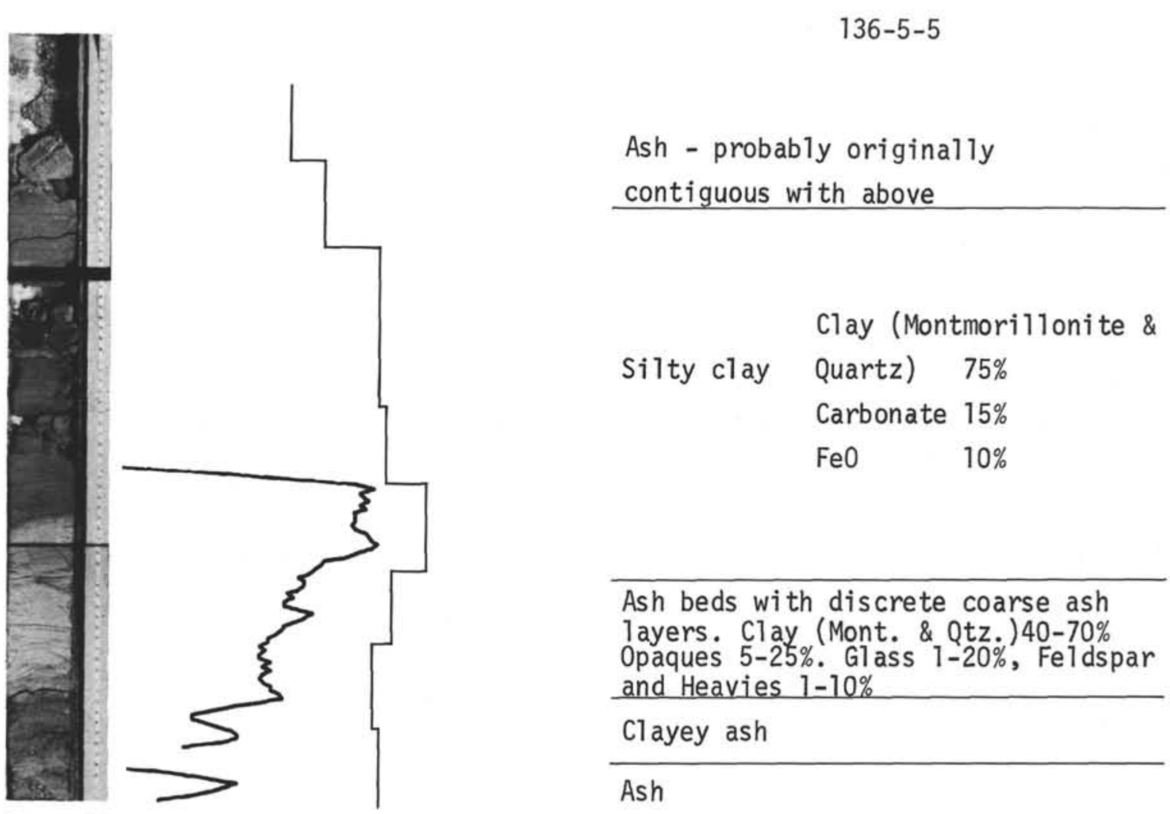
136-5-5
Ash - probably originally contiguous with above
Silty clay
Clay (Montmorillonite & Quartz) 75%
Carbonate 15%
FeO 10%
Ash beds with discrete coarse ash layers. Clay (Mont. & Qtz.)40-70% Opaques 5-25%. Glass 1-20%, Feldspar and Heavies 1-10%
Clayey ash
Ash

Figure 11.

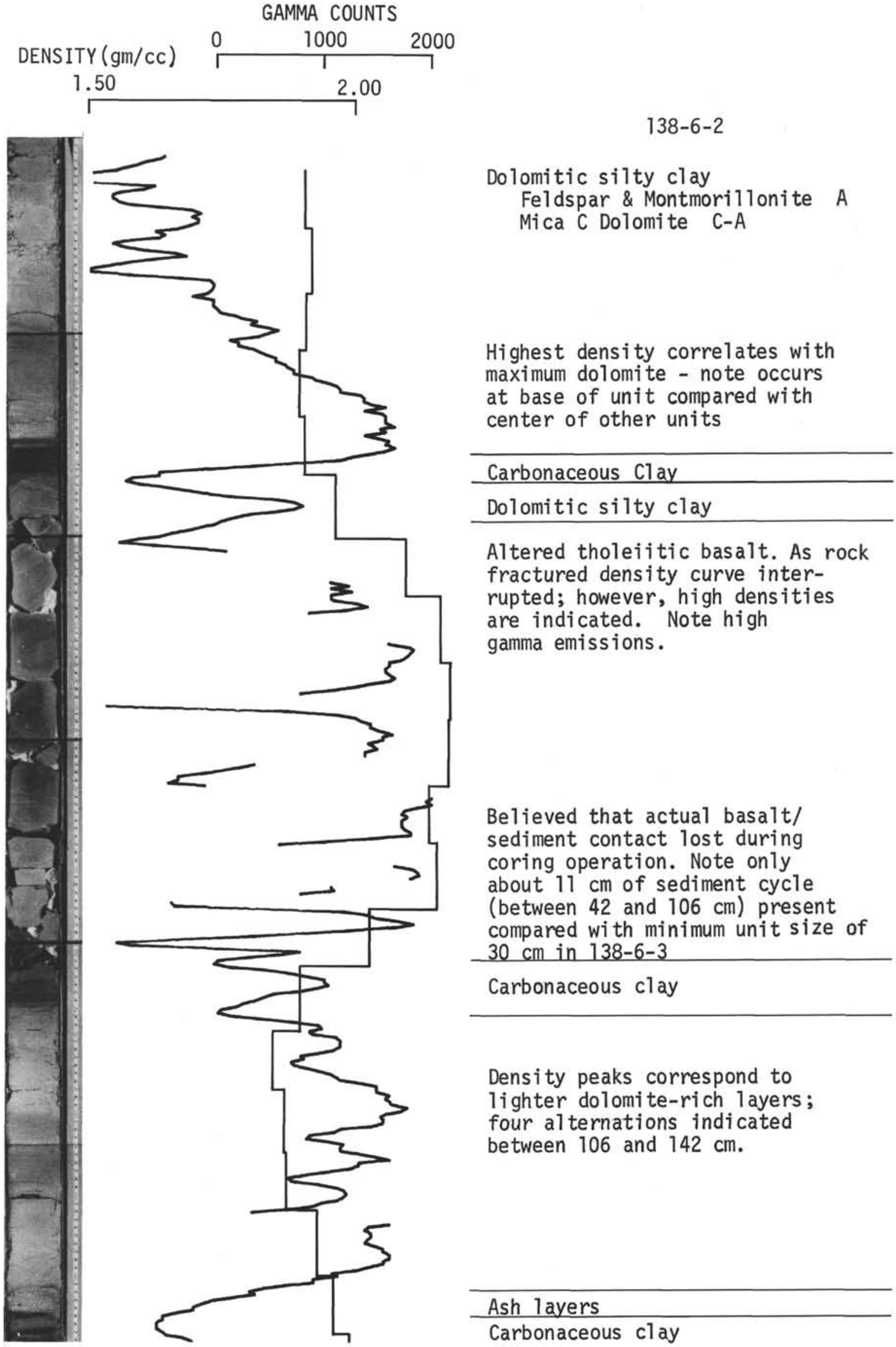
GAMMA COUNTS
0
1000
2000
DENSITY (gm/cc)
1.50
2.00
138-6-2
Dolomitic silty clay
Feldspar & Montmorillonite A
Mica C Dolomite C-A
Highest density correlates with maximum dolomite - note occurs at base of unit compared with center of other units
Carbonaceous Clay
Dolomitic silty clay
Altered tholeiitic basalt. As rock fractured density curve interrupted; however, high densities are indicated. Note high gamma emissions.
Believed that actual basalt/sediment contact lost during coring operation. Note only about 11 cm of sediment cycle (between 42 and 106 cm) present compared with minimum unit size of 30 cm in 138-6-3
Carbonaceous clay
Density peaks correspond to lighter dolomite-rich layers; four alternations indicated between 106 and 142 cm.
Ash layers
Carbonaceous clay

Figure 12.

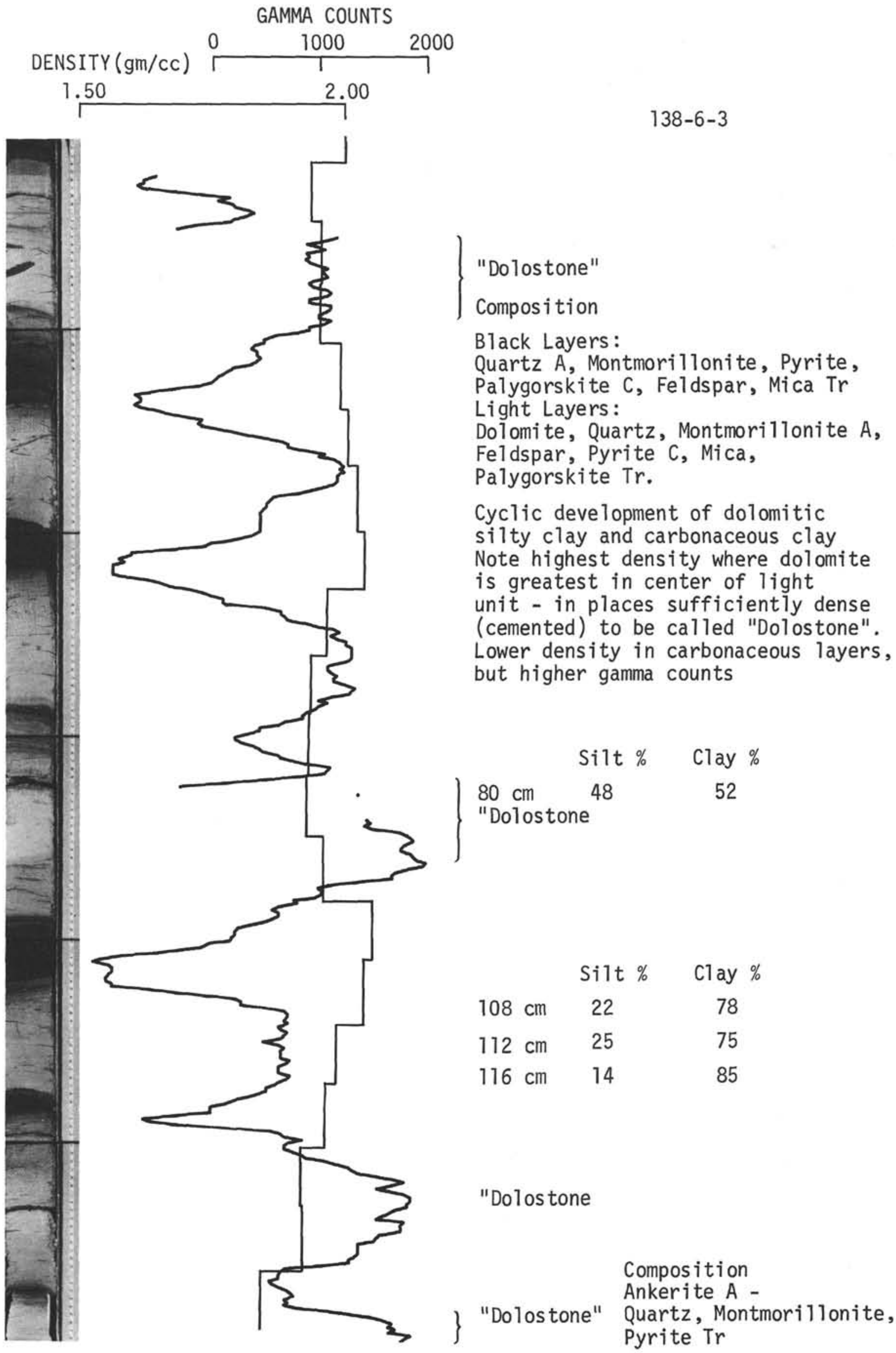
GAMMA COUNTS
0
1000
2000
DENSITY (gm/cc)
1.50
2.00
138-6-3
"Dolostone"
Composition
Black Layers:
Quartz A, Montmorillonite, Pyrite, Palygorskite C, Feldspar, Mica Tr
Light Layers:
Dolomite, Quartz, Montmorillonite A, Feldspar, Pyrite C, Mica, Palygorskite Tr.
Cyclic development of dolomitic silty clay and carbonaceous clay Note highest density where dolomite is greatest in center of light unit - in places sufficiently dense (cemented) to be called "Dolostone". Lower density in carbonaceous layers, but higher gamma counts
Silt % Clay %
80 cm 48 52
"Dolostone
Silt % Clay %
108 cm 22 78
112 cm 25 75
116 cm 14 85
"Dolostone
Composition
Ankerite A - Quartz, Montmorillonite, Pyrite Tr
"Dolostone"

Figure 13.

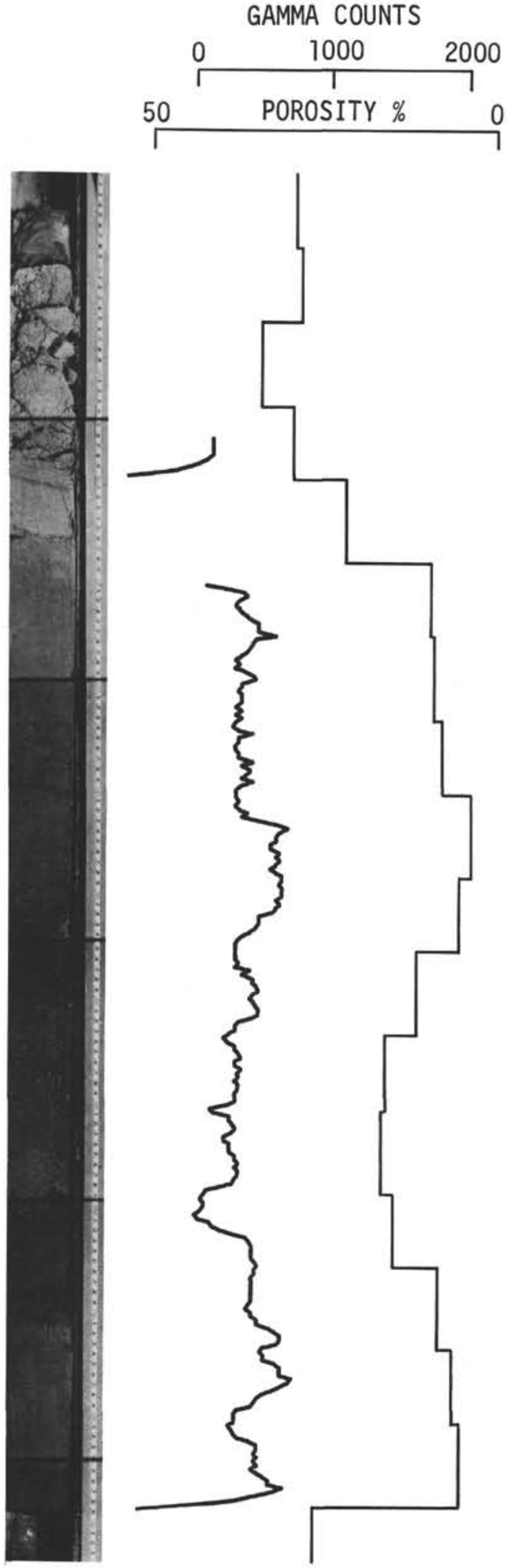

142-5-1

Calcareous clay displaced by drilling

Sand%	Silt%	
66	16	Foram sand-note low gamma counts
81	5	Forams 35%, Nannos 20% Carbonate frags. 25%
74	10	Mica, quartz, FeO, Opaques 20%

Calcareous clay with Mn laminae

–Drilling break–

Silty clay - note high gamma increasing downwards, porosity decreases downwards: this due to increase of $CaCO_3$ upwards, color also lightens

Clay minerals 50-60%
Nannos 10-20%
Carbonate frags. 5-10%
Pyrite, Mica, Quartz 5-10%

17% $CaCO_3$

Sand%	Silt%	
8	74	Graded clayey silt/ sandy silt. Note higher gamma than foram sand, lower than silty clay.
43	44	Porosity increases slightly downwards. Quartz 30%, Clay minerals 20%, Foram
40	47	nanno. & carb. frags. 25%. Rest - chlorite, feldspar, FeO, opaques, heavies & biotite

Clay grading down to silty clay

Figure 14.

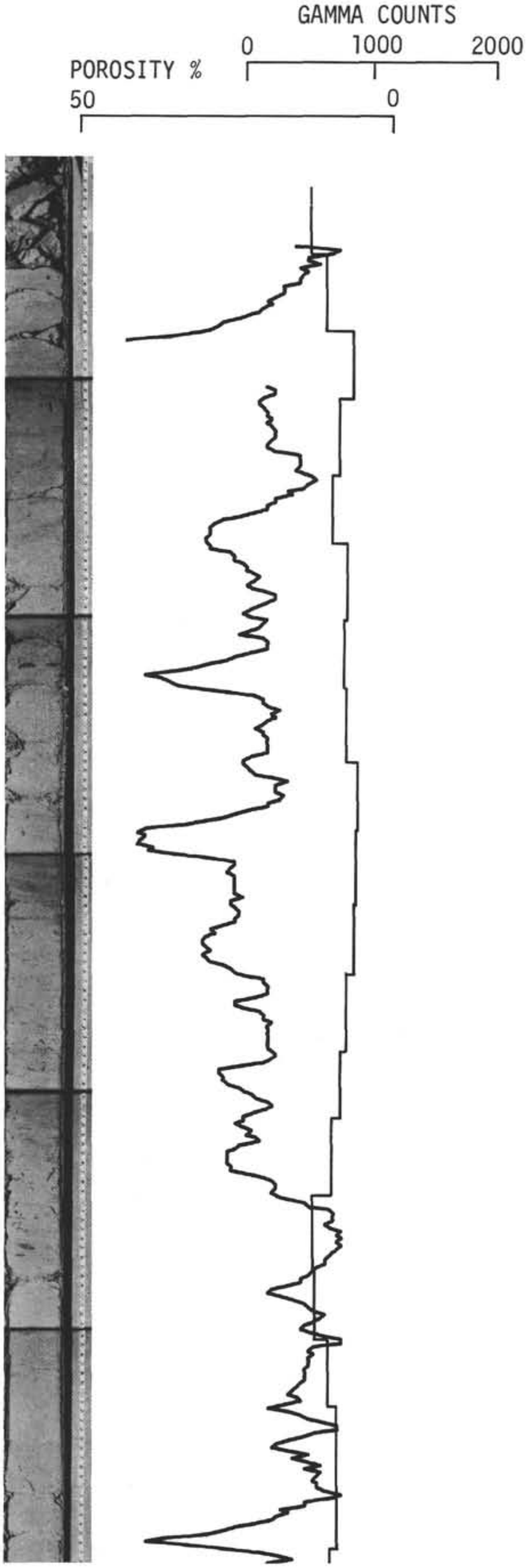

144A-3-1

Foraminiferal nannoplankton chalk ooze

Gamma curve indicates fairly uniform composition - slight variations due to minor components such as zeolite, chlorite-mica.

Nanno 60%, Foram 30%,
Zeolite 5%
Chlorite-mica, pyrite, quartz,
Rads. 5%

Rapid changes in porosity due to varying consolidation. Possibly this is related to activity of burrowing organisms which are restricted to definite zones; the burrows are mostly horizontal and contain disseminated pyrite grains.

Figure 15.

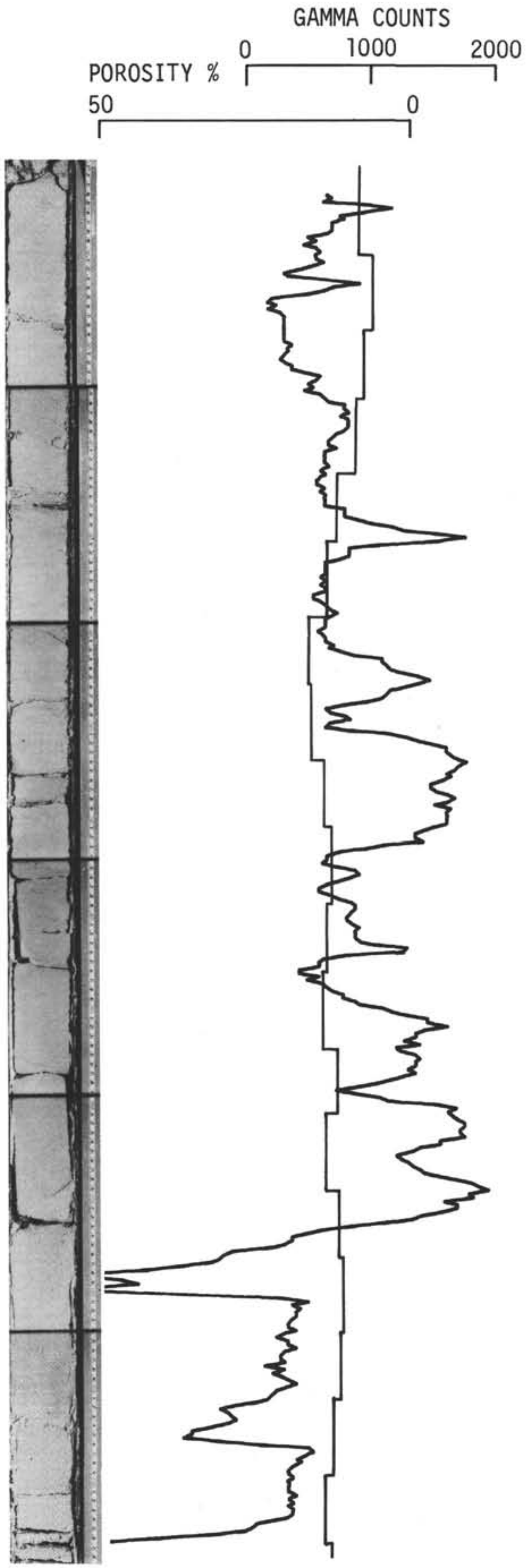

144A-3-2

Foraminiferal nannoplankton marl/chalk ooze
Minor variations in clay and zeolite content indicated by gamma curve.
Porosity values are low because sediment highly indurated ($<5x10^{-1mm}$ penetrometer) except from 113-148 cm where unconsolidated. Note few pronounced spikes indicating very low porosity - at depth of 40 cm spike coincides with lense of small (0.1-0.2 mm) pyrite cubes grown together. Similar composition to 144A-3-1 but mottling and burrowing less pronounced

Note: in several places porosity curve goes below zero - the grain density here is greater than section average of 1.852 used for calculating porosity.

Figure 16.

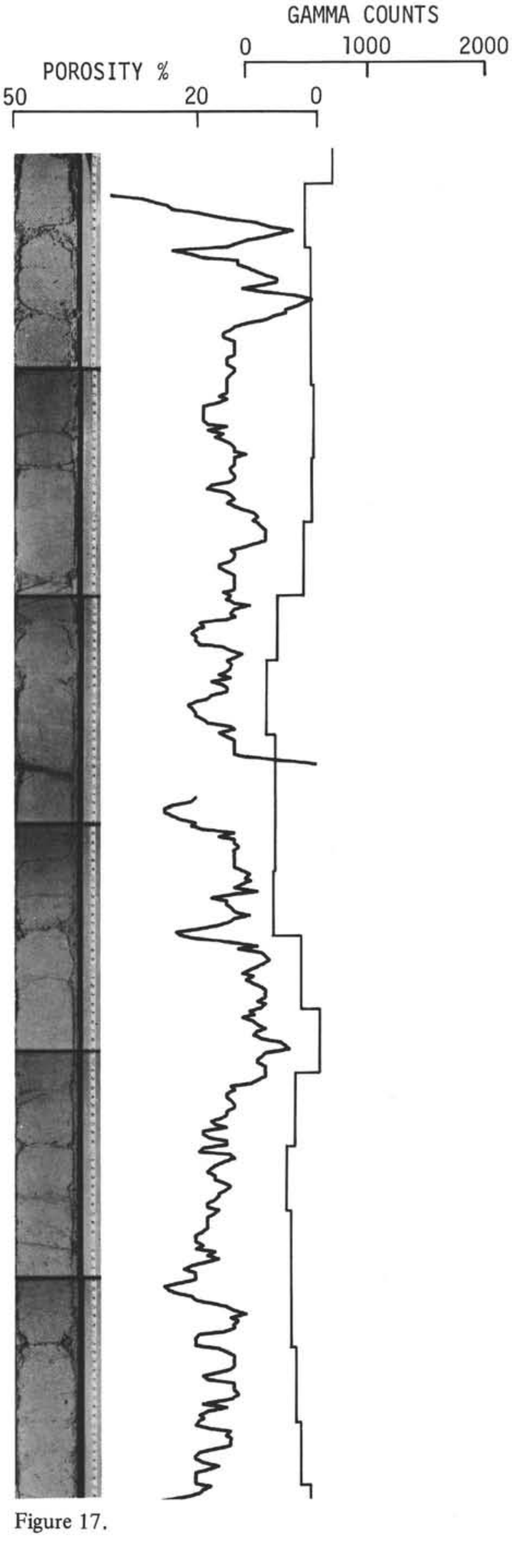

144A-3-5

Zeolite foraminiferal nannoplankton chalk/marl ooze
Faintly mottled, also darker horizontal burrows
Nanno 30%, Foram and Carbonate fragments 25%, Zeolite 15%, Rest - clay minerals, some pyrite, quartz, chlorite

Time hiatus of 8-9 m.y.

At Tertiary/Cretaceous boundary Thanetian stage of Paleocene rests on M. Maestrichtian
Interval 86-102 cm beneath hiatus shows increase in gamma emission and decrease in porosity

Figure 17.